R&D Activities in Airborne SAR Image Processing/Analysis at Lockheed Martin Canada

L. Gagnon[1,2], H. Oppenheim[2], P. Valin[1,2]

[1]R&D Department, Lockheed Martin Canada, 6111 Ave Royalmount, Montréal, H4P 1K6, CANADA
[2]Centre de Recherches Mathématiques, Univ. de Montréal, C.P. 6128 Succ. Centre-Ville, Montréal, H3C 3J7, CANADA

ABSTRACT

We give an overview of some R&D projects in SAR imagery at Lockheed Martin Canada. These projects are motivated by airborne surveillance applications such as the landmass and coastal surveillance missions of the Canadian CP-140 (Aurora) aircraft. The activities reviewed here are 1) R&D supports to CP-140 Spotlight SAR upgrade, 2) fast multiresolution pre-screening filter for CFAR detection, 3) comparison of traditional and wavelet-based speckle filters and 4) high-level ship classification in high-resolution SAR imagery.

1. INTRODUCTION

The R&D Department at Lockheed Martin Canada (LM Canada) is developing SAR image processing/analysis algorithms in the context of airborne surveillance, in collaboration with University partners (Montréal and Queens) and the Department of National Defence (DND). The aim of this paper is to review 4 of these projects: 1) R&D supports to the Spotlight SAR upgrade of the AN/APS-506 radar on-board the Canadian CP-140 (Aurora) aircraft, and design and validation of 2) a fast multiresolution pre-screening filter for CFAR detection, 3) a wavelet-based speckle reduction filter[1,2] and 4) a hierarchical ship classifier for high-resolution Spotlight and/or Inverse SAR imagery[3-6].

In addition to the above, other R&D activities regarding infrared features extraction and video sequence stabilization[7] in FLIR imagery are also performed in collaboration with Montréal and Laval Universities but will not be reported here. All the results of the imaging activities at LM Canada are potentially applicable to landmass or coastal surveillance missions of the CP-140 aircraft.

2. R&D SUPPORTS TO CP-140 SPOTLIGHT SAR UPGRADE

LM Canada is the prime contractor of the Spotlight SAR upgrade to the AN/APS-506 radar on-board the maritime surveillance aircraft CP-140 (Aurora). As such, it heads an industrial group consisting of Array Computing Systems, Raytheon Canada, Applied Analytics, and the IMP Group, in developing the Advanced Demonstration Model (ADM) of the SAR. The ADM is capable of producing high resolution imagery in 4 processing modes, namely StripMap for land imagery, Range Doppler Profiling of naval targets and two Spotlight modes of operation: adaptive for moving naval targets and non-adaptive for stationary land targets.

LM Canada's R&D Department is involved in the algorithmic design review, the acceptance of simulation results, including the important Motion Compensation (MoComp) component, as well as final integration and test of the ADM, and particularly in fine-tuning the crucial Phase Gradient Algorithm (PGA) for final autofocus of residual MoComp errors. Because the target computing platform consists of seven quad boards of Mercury i860s, parallel processing techniques familiar to R&D staff are used throughout and impact the design and repartition of range and azimuth slave processors. This is particularly true of the autofocus component which must sample the complex imagery throughout the Strip being imaged without unduly redistributing the data amongst the workers. The consequences of such restrictions impact on the efficiency of the PGA algorithm in ways which are presently being modeled.

The ADM uses several novel techniques including the unique step transform algorithm for Spotlight imagery, which also incorporates extra tracking features in the Adaptive mode for naval targets. The ADM also features the first implementation of the D^2 algorithm, which is a DREO-proprietary higher order resampling technique that preserves fine-resolution land StripMap imagery at large off-track acquisition (up to 60 degrees forward and 30 degrees backward squint). Since the first in-flight ADM images are expected near the end of 1998, the first results from the StripMap land target detector and the 4-step Sea Spotlight SAR classifier are expected at the start of 1999. Those results, in particular the attribute information

Presented at the International Conf. on Applications of Photonic Technology III
Proceedings SPIE #3491, Ottawa, July 1998, p. 998-1003

relevant to specific platforms in the PDB, will then feed into the MSDF function which will be optimized through this first use of real data (rather than the presently used simulated data).

3. MULTIRESOLUTION PRESCREENING FOR TARGET DETECTION

Efficient target detection schemes in SAR imagery are based on a hierarchical approach where each step in the hierarchy operates on a smaller amount of data with algorithms of increasing computational complexity. Early steps perform low-complexity rejection (prescreening) of nontarget areas while subsequent steps refine the detection (or classification) using, for instance, feature-based false-alarm discrimination. In collaboration with Université de Montréal, LM Canada is investigating a practical multiresolution prescreener for target detection in uniform clutter, based on a wavelet encoding of the scene together with adaptive subband Constant False Alarm Rate (CFAR) detectors. The basic assumption is that man-made objects are easily detectable at low resolution because their scattering is more persistant than for natural objects. Other more sophisticated multiresolution CFAR detectors (prescreeners) are being proposed in the litterature[8,9] but we believe the one presented here has the potential to offer a good trade-off between algorithm complexity and low false alarm (false ROI) rate, while reducing the computational load.

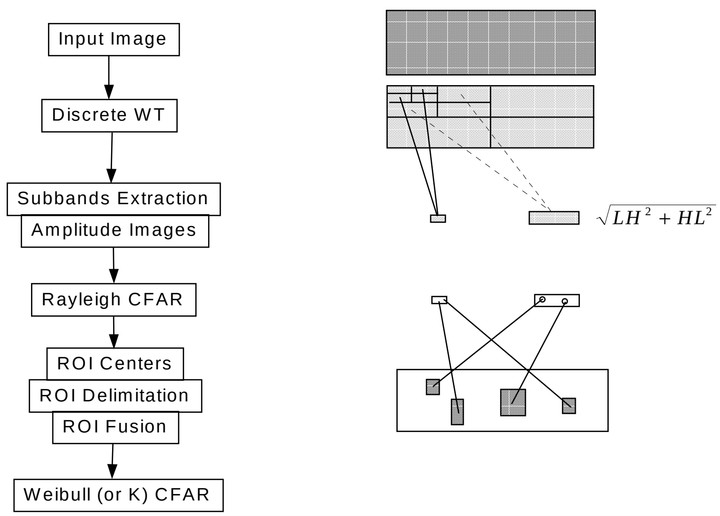

Figure 1: Flow chart of the proposed multiresolution prescreening algorithm suite

With reference to Figure 1, the detector under investigation involves the following steps:

- The input image (a wide area StripMap SAR image) is multiresolution-encoded using a discrete wavelet transform based on symmetric real filters like the bi-orthogonal wavelets. Even and odd parities of such filters allow reflection-like boundary extension at image boundaries and facilitate the subsequent ROI positioning.
- A set of small low-resolution images is then formed using the Low-High (LH) and High-Low (HL) blocks in one or few adjacent resolution levels. The choice and number of levels depend on the *a priori* spatial target extent the operator is looking for. The set of low resolution images is formed by the vector sum of the wavelet coefficients in the LH and HL blocks for each selected resolution level. The presence of a target in the initial image should be reflected by an intense pixel in at least one of the amplitude images.
- A CFAR detection is applied to the amplitude image based on the assumption that the wavelet coefficients in blocks LH and HL both follow Normal distributions of same variance, which yields a Rayleigh distribution for the vector amplitude of the two components. This assumption is approximatively true in practice, provided the clutter is homogeneous. Following the CFAR theory for Rayleigh distribution[10], a pixel is declared to pass the CFAR detection test (i.e. to belong to the signal rather than the clutter) if its intensity exceeds a threshold T given by

$$T = \alpha B \qquad B = \sqrt{\frac{1}{M}\sum_{i=1}^{M} x_i^2} \qquad P_{FA} = \left(1 + \frac{\alpha^2}{M}\right)^{-M}$$

where M is the number of neighborhood pixels over which the Rayleigh distribution parameter B is estimated and P_{FA} is the assigned probability of false alarms. As usual in spatial matched filtering applications, pixel statistics is calculated over a square annulus centered on the test pixel. The annulus dimension can be very small since the targets dimension is also very small at these low resolutions.

- In our implementation, the Rayleigh CFAR is applied twice: a first pass to detect very intense pixels using a high P_{FA} that serve as a seed to a second pass that detect neighborhood pixels above a second, but lower, P_{FA}. The amplitude image pixels that pass the two-pass detection are used to identify ROIs in the initial image. A square ROI is assigned to each of these pixels, for which the dimension is a function of the *a priori* targets dimension. In addition, the ROI positioning is weighted according to the intensity of the neighborhood pixels in the low-resolution amplitude image.
- Two ovelapping elementary ROIs are clustered in one larger ROI as they could correspond to a large target in the original image that does not appear “point-like” at the selected resolution.
- Once all ROIs have been detected and clustered, the operator can apply the CFAR detector that is appropriate to the clutter statistics of the scene (for instance, Weibull[10] and K distribution for ground and sea clutter, respectively). Combination of ROI center CFAR detection in low spectral bands and CFAR detection in ROIs, result in a drastic reduction in the computational load, compared to a usual CFAR detection in the entire image.

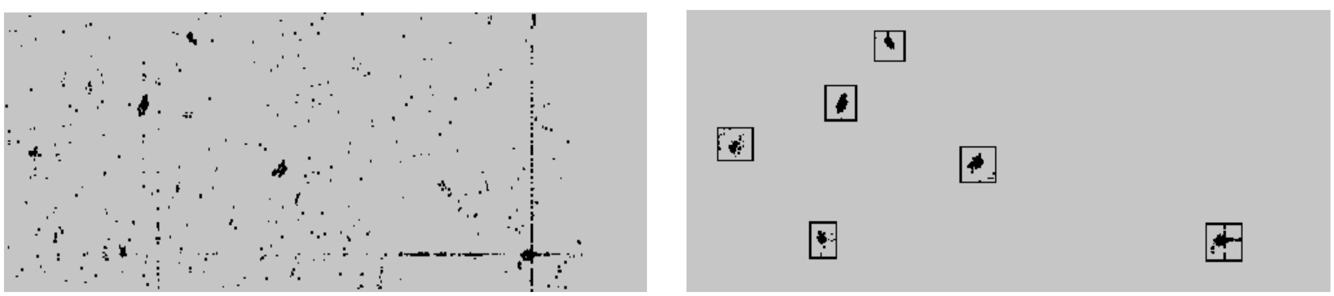

Figure 2: Example of ROI detection without (left) and with (right) an intermediate Rayleigh CFAR detection at level 4

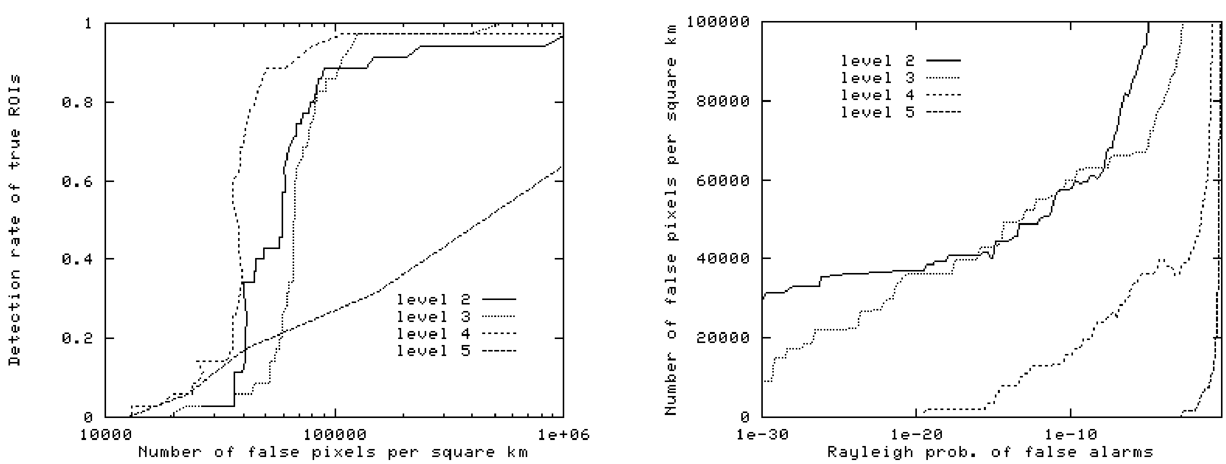

Figure 3: ROC curves (left) and false pixels detection rate (right) summarizing algorithm performance when applied to the detection of tanks and trucks in one-foot resolution HH-polarization SAR imagery

We have tested our algorithm on a publicly available subset of the one-foot resolution MIT-ADTS (Advanced Detection Technology Sensor) SAR images. The subset contains 12 HH-polarization armored land scenes (tanks and trucks). Figure 2 shows the ROI detection result obtained on this type of imagery without and with an intermediate Rayleigh CFAR detection performed at level 4.

Preliminary measures of detection performance are summarized by the graphics shown in Figure 3. These are obtained from the 7 (out of 12) images for which the ground truth is known. Figure 3-left are Receiver Operating Characteristic curves showing the probability of detecting a target (i.e. a ROI with a true target in it *after* ROI clustering) as function of the number of false alarms (i.e. the total number of pixels in the false ROIs) for detection at levels 2, 3, 4 and 5. The few unusual local decreases in the number of false pixels along curves in Figure 3-right is the result of clustering false ROIs with true ones. This explains the few local bias towards the left in the corresponding ROC curves (Figure 3-left). Figure 3-left shows that the detection performance is globally better at level 4 (i.e. best detection to false alarm ratio), which turns out to be the most appropriate resolution level for the dimension of targets present in the scenes. In addition, the processing time is about 3 times faster than at level 2.

4. SPECKLE REDUCTION

Speckle is a common phenomena in all coherent imaging systems like laser, acoustic and SAR imagery. It is often an undesirable effect, especially in Automatic Target Recognition (ATR) systems. Various standard filters are used to process speckle. Among them are the Median, Lee, Kuan, Frost, Gamma, Geometric, Oddy and AFS (Adaptive Filter on Surfaces).

	S/MSE
Noisy	4.4
Kuan	14.0
Gamma	14.1
Frost	14.6
Geometric	13.8
Oddy	14.3
Wavelet	16.3

Table 1: Quantitative enhancement performance on the simulated noise

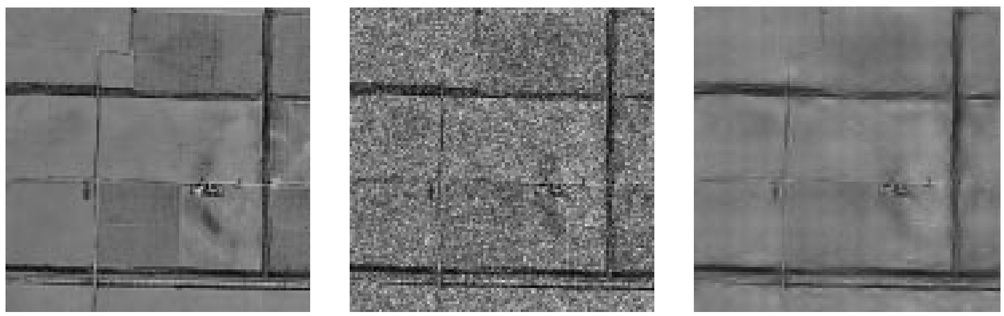

Figure 4: Original (left), noisy (middle) and wavelet-filtered image (right)

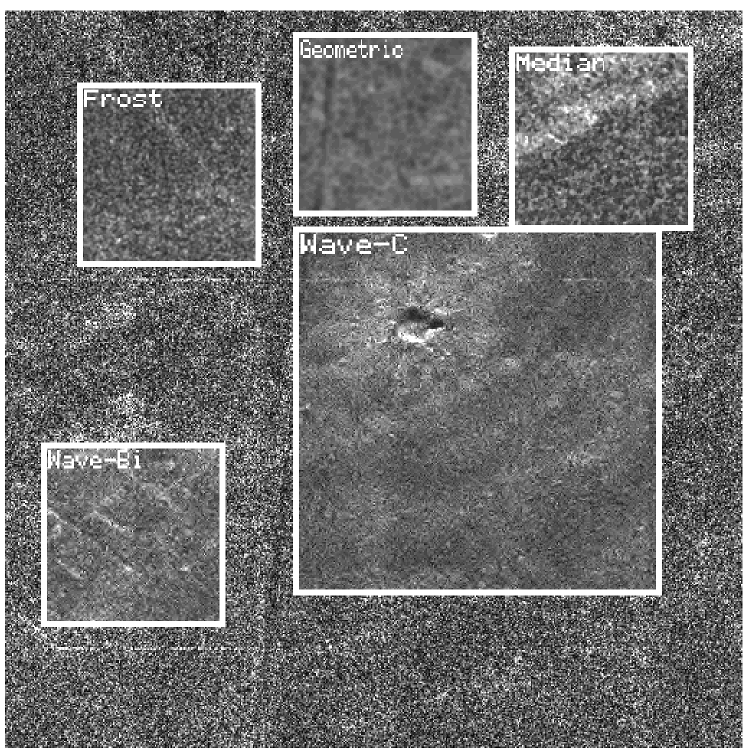

Figure 5: Examples of speckle filters on a real image using custum and wavelet filters (bi-orthogonal and SD wavelets)

All these filters usually perform well on most SAR images but with some limitations regarding resolution degradation and smoothing of uniform areas. Wavelet-based filters have been proposed to overcome these difficulties. They are all based on the Wavelet Coefficient Shrinkage (WCS) principle, i.e. the thresholding of wavelet coefficients that are associated to noise. LM Canada has proposed such a filter[1,2], based on the use of the Symmetric Daubechies (SD) wavelets[11]. In addition to sharing the same properties as the standard Daubechies wavelets (i.e. compact support, orthogonality and vanishing moments), SD wavelets and scaling functions are symmetric and have a better interpolation capability.

Our wavelet-based speckle filter makes use of the well-known soft-thresholding procedure, modified in order to manage the complex-valued properties of the SD wavelet coefficients. The basic hypothesis is that, for each spectral band (the so-called LH, HL and HH blocks), the complex wavelet coefficients follow a non-diagonal bi-Normal distribution (real and imaginary parts are correlated). In addition, the distributions are usually oriented differently in each block. Thus, our algorithm performs WCS with respect to the principal axes, taking care of preserving the eccentricity and orientation of the 2-D distributions. As a result, this leads to a type of non-linear WCS procedure where the threshold level depends on the phase of each wavelet coefficient. This algorithm has been tested against the above custom speckle removal filters and has been shown to outperform them qualitatively and quantitatively, especially for high-level noise, in terms of Signal-to-Mean-Square-Error (S/MSE) ratio and Equivalent Number of Looks (ENL). Table 1 gives the various S/MSE obtained after filtering an optical image (Figure 4-left) with simulated speckle noise. The noise level correspond to the Number of Looks of 2.7 (Figure 4-middle). Figure 4-right is the enhanced image after our WCS filtering. Figure 5 shows various results obtained on a real SAR image from the public Multi-Sensor Pod program (www.amps.gov) after Frost, Median, Geometric and 2 wavelet-based filters based on bi-orthogonal and SD wavelets.

5. SHIP RECOGNITION IN HIGH-RESOLUTION SAR IMAGERY

Image resolution refinements in modern radar now make possible the use of SAR for the detection and recognition of naval vessels. Technically, the problem is complex because of numerous practical issues like uncontrolled environment, variable 3-D image acquisition geometry, image blurring due to ship motion, speckle noise, dependence of radar scattering to ship orientation, etc.

The R&D Department at LM Canada has started addressing this problem 3 years ago where we engaged IRAD activities on ship classification in collaboration with University partners (Queens and Montréal Universities) with the aim of acquiring technical expertise in this field. More recently (1997), LM Canada was awarded a DND contract for which one of the main objectives is the design, implementation and test of a viable high resolution SAR-based ship classification module within a CP-140 Multi Sensor Data Fusion (MSDF) design.

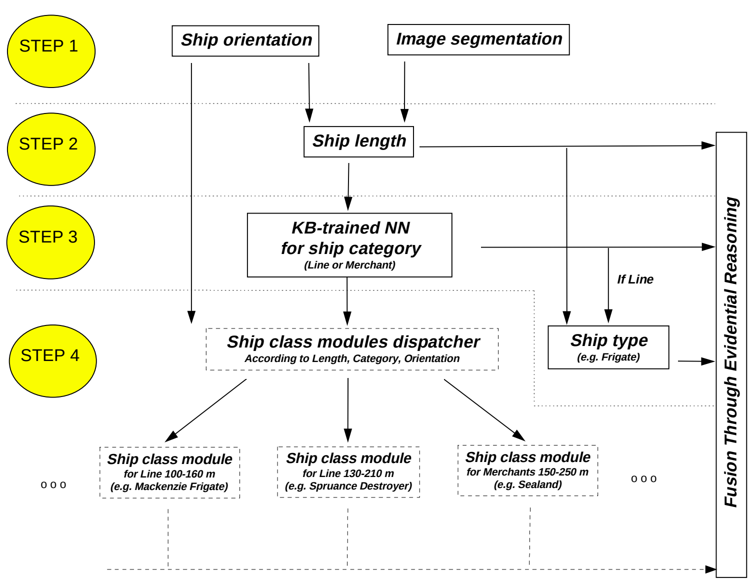

Figure 6: High-level design of the ship classifier under investigation

LM Canada has proposed and is currently evaluating a practical ship classification approach applicable to SpotSAR and ISAR imagery acquired from an airborne platform (Figure 6). The classifier uses a hierarchical approach for feature extraction and target identity declaration. The algorithm performs the following steps: 1) target segmentation, 2) ship length extraction, 3) ship classification according to category (Line, i.e. military combatant and Merchant) and type (e.g. Frigate, Destroyer, Cruiser, etc.) and 4) ship class declaration (e.g. Mackenzie Frigate, Spruance Destroyer, etc.). Each of these informations is sent as a target attribute to a Multi Sensor Data Fusion system. Segmentation is based on a combination of directional pixel intensity thresholding and small regions merging. Extraction of ship length is performed using a Hough transform that identifies the ship center-line. Ship category declaration is obtained through the use of a knowledge-based-trained Back-Propagation Neural Network (BP-NN) that analyzes the spatial distribution of radar scatterers in 9 sections of the ship. Ship type declaration is done through a Bayes classifier based on the ship length. Finally, various NN architectures for ship class declaration are under investigation, including multiresolution BP-NN. Many of these techniques were inspired of, or simultaneously proposed in other articles and reports[12-14].

At this time, the testbed is able to extract ship length attribute and provide estimates (with confidence level) of ship category and Line ship type (Frigate, Destroyer, Cruiser, Battleship or Aircraft Carrier) for long range SpotSAR and ISAR imagery. In its current version, the system performance can be qualified as adequate for use within a MSDF architecture and fair for use as a stand alone decision-aid module (see Ref. [5] for more details).

6. ACKNOWLEDGEMENTS

These activites are supported by 1) Internal R&D funds at LM Canada, 2) the Canadian Department of National Defence under contracts #W7701-6-4081 and #W8477-4-YG02/01-QF and 3) the Natural Science and Engineering Research Council (NSERC) of Canada under grants to collaborating Universities. Special thanks to A. Jouan from LM Canada, S. Blostein and H. Osman from Queens University, F. Drissi-Smaili and V. Gouaillier from Université de Montréal, J. Campbell from the Defence Research Establishment Ottawa and E. Bossé from the Defence Research Establishment Valcartier.

7. REFERENCES

1. L. Gagnon, F. Drissi Smaili, “Speckle Noise Reduction of Airborne SAR Images with Symmetric Daubechies Wavelets”, *SPIE Proc. #2759*, pp. 14-24, 1996
2. L. Gagnon, A. Jouan, “Speckle Filtering of SAR Images - A Comparative Study Between Complex-Wavelet-Based and Standard Filters”, *SPIE Proc.* #3169, pp. 80-91, 1997
3. H. Osman, S. Blostein, L. Gagnon, “Classification of Ships in Airborne SAR Imagery Using Backpropagation Neural Networks”, *SPIE Proc. #3161*, pp. 126-136, 1997
4. V. Gouaillier, L. Gagnon, “Ship Silhouette Recognition Using Principal Components Analysis”, *SPIE Proc. #3164*, pp. 59-69, 1997
5. L. Gagnon, R. Klepko, “Hierarchical Classifier Design for Airborne SAR Images of Ships”, *SPIE Proc. #3371*, 1998
6. A. Jouan, L. Gagnon, E. Shahbazian, P. Valin, “Fusion of Imagery Attributes with Non-Imaging Sensor Reports by Truncated Dempster-Shafer Evidential Reasoning”, FUSION’98, Las Vegas, July 1998
7. D. McReynolds, Y. Sheng, L. Gagnon, L. Sévigny, “Stabilization of Infrared Sequence With Computer Vision Techniques”, this ICAPT conference, 1998
8. W. Irving, L. Novak, A. S. Willsky, “A Multiresolution Approach to Discrimination in SAR Imagery”, IEEE Trans. AeroSpace and Electron. Systems, Vol. 33, No 3, pp. 1157-1168, 1997
9. N. S. Subotic, B. J. Thelen, J. D. Gorman, M. F. Reiley, “Multiresolution Detection of Coherent Radar Targets”, IEEE Trans. Image Processing, Vol. 6, No. 1, pp. 21-35, 1997
10. R. Ravid, N. Levanon, “Maximum-Likelihood CFAR for Weibull Background”, *IEE Proceedings-F*, Vol 139, No. 3, pp. 256-264, 1992
11. J. M. Lina, M. Mayrand, “Complex Daubechies Wavelets”, App. Comp Harmonic Anal., Vol. 2, pp. 219-229, 1995
12. R. J. Drazovich, F. X. Lanzinger, T. O. Binford, “Radar Target Classification”, *Proc. IEEE PRIP ’81*, pp. 496-501, 1981
13. S. Musman, D. Kerr, C. Bachmann, “Automatic Recognition of ISAR Ship Images”, *IEEE Trans. Aerospace Electronic Systems*, Vol. 32, pp. 1392-1403, 1996
14. M. Menon, “An Automatic Ship Classification System for ISAR Imagery”, *SPIE Proc. #2492*, pp. 373-388, 1995